International Journal of Sediment Research 33 (2018) 27–34

Contents lists available at ScienceDirect

International Journal of Sediment Research

journal homepage: www.elsevier.com/locate/ijsrc

Original Research

Near-bankfull floods in an Alpine stream: Effects on the sediment mobility and bedload magnitude

Riccardo Rainato [a,*], Luca Mao [b], Lorenzo Picco [a]

[a] Department of Land, Environment, Agriculture and Forestry, University of Padova, Padova, Italy
[b] Department of Ecosystems and Environment, Pontificia Universidad Catòlica de Chile, Santiago, Chile

ARTICLE INFO

Article history:
Received 5 September 2016
Received in revised form
9 February 2017
Accepted 26 March 2017
Available online 30 March 2017

Keywords:
Bedload
Alpine basin
Sediment dynamics
Bedload tracing
PIT-tags

ABSTRACT

In a mountain environment, the transport of coarse material is a key factor for many fields such as geomorphology, ecology, hazard assessment, and reservoir management. Despite this, there have been only a few field investigations of bedload, in particular using multiple monitoring methods. In this sense, attention has frequently focused on the effects of "high magnitude/low frequency floods" rather than on "ordinary events". This study aims to analyze the sediment dynamics triggered by three high-frequency floods (recurrence interval "*RI*" between 1.1 and 1.7 yr) that occurred in the Rio Cordon basin during 2014. The flood events were investigated in terms of both sediment mobility and bedload magnitude. The Rio Cordon is an Alpine basin located in northeastern Italy. The catchment has a surface area of 5 km^2, ranging between 1763 and 2763 m above sea level. The Rio Cordon flows on an armored streambed layer, with a stable step-pool configuration and large boulders. Since 1986, the basin has been equipped with a permanent station to continuously monitor water discharge and sediment flux. To investigate sediment mobility, 250 PIT-tags were installed in the streambed in 2012. The 2014 floods showed a clear difference in terms of tracer displacement. The near-bankfull events showed equal mobility conditions, with mean travel distance one order of magnitude higher than the below-bankfull event. Furthermore, only the near-bankfull events transported coarse material to the monitoring station. Both events had a peak discharge up to 2.06 m^3 s^{-1}, but the bedload transport rates differed by more than one order of magnitude, proving that under the current supply-limited condition, the bedload appears more related to the sediment supply than to the magnitude of the hydrological features. In this sense, the results demonstrated that near-bankfull events can mobilize large amounts of material for long distances, and that floods of apparently similar magnitude may lead to different sediment dynamics, depending on the type and amount of sediment supply.

1. Introduction

Bedload transport in mountain streams strongly affects downstream sediment delivery (Liébault et al., 2016), channel stability (Baewert & Morche, 2014), and, thus, the assessment of hazard areas along river corridors. Within the context of the European Union (EU) water framework directive, an accurate assessment of sediment transport is required for flood risk mapping and management. Also, from an ecological point of view, in many mountain regions the spawning habitats of fishes and the lifecycle of micro- and macro-invertebrates appear to be strongly affected by bedload (Vazquez-Tarrio & Menendez-Duarte, 2014; Wohl, 2015). However, bedload is notoriously difficult to measure in the field as the high-energy and impulsive nature of bedload make its investigation and assessment a challenging task. This is particularly evident in mountain streams, where several factors make bedload processes differ from those in lowland rivers. In addition to the high gradient, sediment mobility is strongly influenced by the highly heterogeneous streambed material, which results in factors such as grain sorting (Hammond et al., 1984), particle size interactions and hiding-protrusion effects (Ashworth & Ferguson, 1989), low relative roughness (Bathurst et al., 1983), presence of a strong armor layer (Lenzi, 2004), embedding and exposed patches (Bathurst, 2013), and slope (Lamb et al., 2008). In addition to the magnitude of a flood event (Lenzi et al., 2006a), the bedload transport rate is strongly related to sediment supply conditions (Beylich & Laute, 2015; Downs et al., 2016; Liébault et al., 2012; Recking, 2012; Schwendel et al., 2011), and hillslopes-channel coupling (Cavalli et al., 2013). These complex conditions are

* Corresponding author.
E-mail address: riccardo.rainato@unipd.it (R. Rainato).

http://dx.doi.org/10.1016/j.ijsrc.2017.03.006
1001-6279/

reflected in the poor performance of bedload predictive equations, which are usually derived from laboratory experiments or specific field sites (Yager et al., 2015).

The availability of field data also is quite scarce, with a lack of monitoring programs maintained at the same study site over long periods. Nevertheless, several direct and indirect monitoring methods have been developed in the recent decades, enabling valuable field data to be obtained about bedload (Habersack et al., in press; Krein et al., 2016; Mao et al., 2016; Rickenmann et al., 2012). By collecting the sediment that is transported over a certain time interval, bedload traps allow the rate and grain size of coarse material mobilized to be analyzed (Bunte et al., 2008). The devices can be installed in permanent monitoring stations, enabling analysis over long time scales (Rainato et al., in press), or can be used as moving traps, focusing on short time periods (Mao et al., 2008).

The tracers method consists of individual particles that are collected, painted, and replaced in the channel (Fraley, 2004). Single-grain tracers can be used to investigate sediment travel distances (Olinde & Johnson, 2015), virtual velocity (Houbrechts et al., 2015), bedload transport rates (Dell'Agnese et al., 2015), threshold conditions (Lenzi et al., 2006b) and to estimate bedload volumes during flood events (Liébault & Laronne, 2008; Schneider et al., 2014), and can be integrated with information obtained from traps (Ferguson & Wathen, 1998). Recently, the application of the Radio Frequency Identification technology (RFID) to sediment tracing has allowed buried tracers to be detected, increasing the recovery rates (Lamarre et al., 2005). In particular, to achieve continuous tracing, the particles can be embedded with Passive Integrated Transponders (PIT) programmed with a unique identification code (ID). In terms of investigation, the PIT-tags are small, not too expensive, and can potentially allow long-lasting monitoring. The information obtained from these tracers can be extremely useful since the bedload transport rate in mountain channels seems to depend on width and depth of bed scouring, as well as travel distances of the sediment particles (Schneider et al., 2014).

Here the results obtained from an investigation of near-bankfull floods that occurred in 2014 in the Rio Cordon instrumented basin (Eastern Italian Alps) are presented. Three high-frequency bedload events occurred in May, June, and November. They were investigated in terms of both bedload amount (i.e. coarse material trapped by the monitoring station) and analysis of the displacements of 250 PITs installed along the streambed. Despite the relatively low magnitude of flood events, the complex features that occurred in terms of sediment supply and hydraulic forcing enabled different sediment dynamics to be clearly observed and analyzed.

2. Study area and methods

2.1. Rio Cordon study site

The Rio Cordon basin (Dolomites, northeast Italy) drains a surface of 5 km^2, ranging from 1763 to 2763 m a.s.l. (Fig. 1). Alpine climatic conditions prevail in the watershed, with a prevalent nivo-pluvial runoff regime. The long-term mean annual precipitation is 1150 mm. Quaternary moraines and scree deposits are very common throughout the basin, but are mainly disconnected from the drainage network. In terms of land use, most of the catchment is covered by Alpine grasslands (61%) and shrubs (18%). Barely 7% of the area is forested, while 14% is bare land. Talus slopes, shallow landslides, eroded stream banks, and debris flow channels are the main sediment source areas, covering 5.2% of the basin (Lenzi et al., 2003). Due to distance and the decoupling of such sources, the drainage network normally has a low/moderate

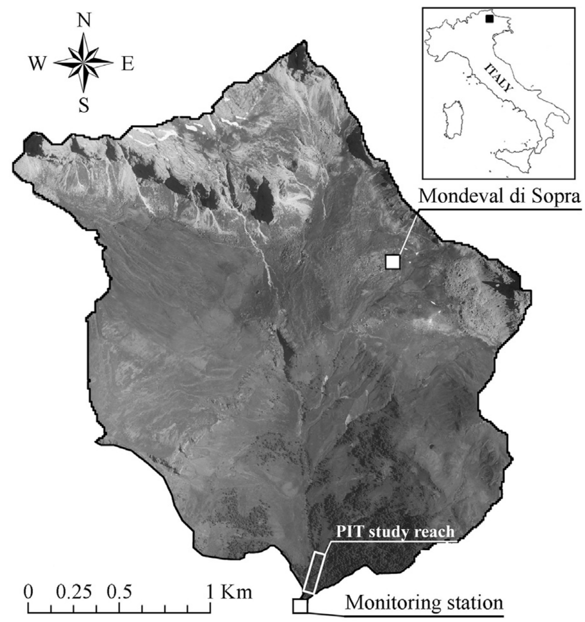

Fig. 1. The Rio Cordon study site. "Mondeval di Sopra" identifies the upstream meteorological station, while "Monitoring station" identifies both the sediment transport monitoring and the downstream meteorological station.

sediment supply. The Rio Cordon has an average slope of 17%, a rough streambed with a step-pool configuration and large boulders. The grain size distribution (GSD) of the streambed surface is characterized by D_{16}=29 mm, D_{50}=114 mm, and D_{84}=358 mm (where D_x means the sediment diameter for which x percent of the sediment is finer). Overall, the stream has a well-developed armor layer, with the sub-surface GSD (D_{50ss}=38 mm) clearly finer than the surface material. Based on field observations, Lenzi et al. (2006a) defined the bankfull discharge as 2.30 $m^3\ s^{-1}$.

Since 1986, a permanent monitoring station has recorded water discharge, bedload and suspended load of the Rio Cordon stream (Fattorelli et al., 1988). The station consists of an inlet flume, an inclined grid, a storage area for bedload material, an outlet flume, and a settling basin for the suspended load material (Picco et al., 2012). The water discharge is measured hourly by two water level gauges and a sharp-crested weir. During flood events, the sampling interval decreases to 5 min. The inclined grid (60% longitudinal slope) enables the coarse sediment ($>$20 mm) to be separated from water and fine material. Once separated, the coarse material sinks into the storage area, where 24 ultrasonic sensors continuously measure the amount transported. Turbidimeters were installed in the inlet and outlet channel to measure the suspended load. Two meteorological stations in the study basin record air temperature, atmospheric pressure, relative humidity, solar radiation and rainfall hourly. The upstream meteorological station "Mondeval di Sopra" is located at 2130 m above sea level, while downstream the climatic conditions are measured at 1763 m a.s.l., in proximity to the monitoring station (Fig. 1). The Rio Cordon instrumented basin is managed by ARPA Veneto, Regional Department for Land Safety.

2.2. Methods

Data collected at the monitoring station were used to analyze the flood events in terms of bedload magnitude. The 5-min interval discharge data were used to describe the hydrological features of the floods, i.e. hydrograph, peak discharge (Q_{PEAK}), and duration of the events. In the case of a bedload event, the effective runoff (ER, $10^3\ m^3$) was also estimated. The effective runoff is

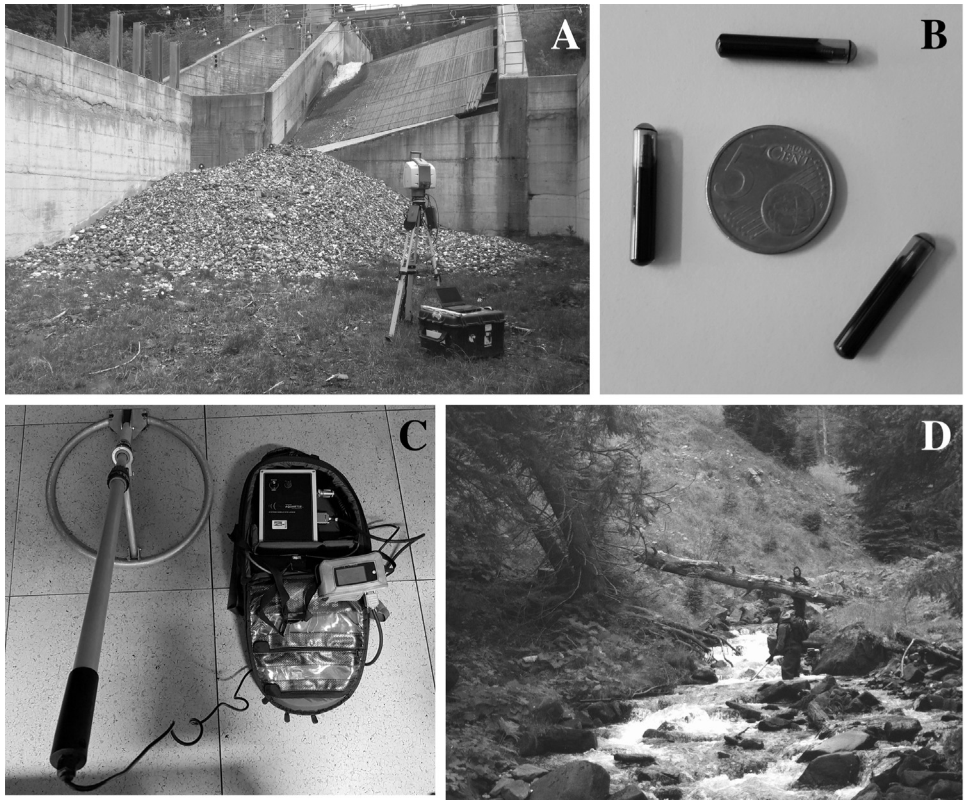

Fig. 2. Storage area during the TLS survey (A), 23-mm PITs (B) and mobile antenna (C) used for the bedload tracing in the Rio Cordon (D).

defined as the portion of hydrograph volume that contributes to the transport. To obtain it, the discharge measurements were compared with the data simultaneously recorded by ultrasonic sensors and turbidimeters, enabling the threshold discharges and the portion of time exceeding the threshold discharge (i.e. *ER*) to be defined. In addition, the data gathered by the meteorological stations were used to define the antecedent climatic conditions, in particular the cumulative rainfall during the 24 (R_{24}) and 48 h (R_{48}) before the event. The amount of bedload transported to the monitoring station (*BL*) was estimated by surveying the storage area after each flood using a Terrestrial Laser Scanner (TLS). Specifically, a Leica ScanStation2® device was used to scan the deposited coarse material (Fig. 2A). The point clouds obtained were managed in the ArcGIS® environment, by creating the Digital Elevation Model and then measuring (Surface Volume tool) the bedload volumes (cell size = 0.02 m). The grain size distribution of the coarse material was also evaluated, using the grid by number approach.

Between 2009 and 2012, 250 particles equipped with 23-mm PITs (Fig. 2B) were seeded on the Rio Cordon streambed to investigate their mobility. The sizes of the particles (*b-axis* = 40–190 mm) were selected in order to be a representative sample of the channel bed. Specifically, the GSD of the tracers matched $D_{25} < D < D_{70}$ of the streambed surface. The PIT-tags were installed along several cross sections, starting from a cascade/step-pool stretch located 318 m upstream of the monitoring station.

When placing the particles equipped with PITs on the channel bed, they were gently pressed down with the heel of the waders to roughly recreate their natural arrangement among the streambed material (Vazquez-Tarrio & Menendez-Duarte, 2014). To monitor the tracer displacements, an Aquartis Accueil® mobile antenna based on RFID technology was used (Fig. 2C). This detection device consists of a control module (kept in a backpack), an LCD display panel (for ID identification) and a loop transponder detection antenna 0.53 m in diameter. It is powered by a 12-volt battery. A laser rangefinder was used (horizontal accuracy = 0.01 m) to measure the distances traveled by the PIT-tags. The field surveys were done by two operators equipped with a mobile antenna and a laser rangefinder (Fig. 2D). Once mobilized, the PIT-tags were not relocated in the release sections but were left where found, leaving them to travel over the entire study reach (318 m). To improve the displacement estimation, the reach was divided into 23 straight stretches and the cross sections that delimited the stretches were used as reference points. Due to the difficult conditions in which the PIT surveys were done (i.e. high-gradient, step-pool and cascade) and the size of the loop antenna (0.53 m), the exact positioning of the tracers could only be measured with some degree of uncertainty. For this reason, only displacements > 1 m were considered in this analysis. Hereinafter, the terms "PIT-tags" or "tracers" are used to identify the particles equipped with passive integrated transponders. The terms "survey" and "inventory" will be used to describe the field-phase in which the PITs were monitored. During 2014, three PIT surveys were performed in the Rio Cordon, on May 15, June 30, and November 24.

3. Results

In terms of climatic conditions, the study period (2014) was characterized by significant snowfalls during the first months of the year that led to an extended snowmelt period (i.e. early April-late June). Typical Alpine climatic conditions were observed in the following months, with frequent rainstorms in summer and persistent rainfalls during autumn (Fig. 3). The highest daily precipitation of the year was recorded on November 5, with 126.2 mm d^{-1} (Fig. 3).

Three high frequency flood events were observed in the Rio Cordon during 2014. First, a below-bankfull event occurred during

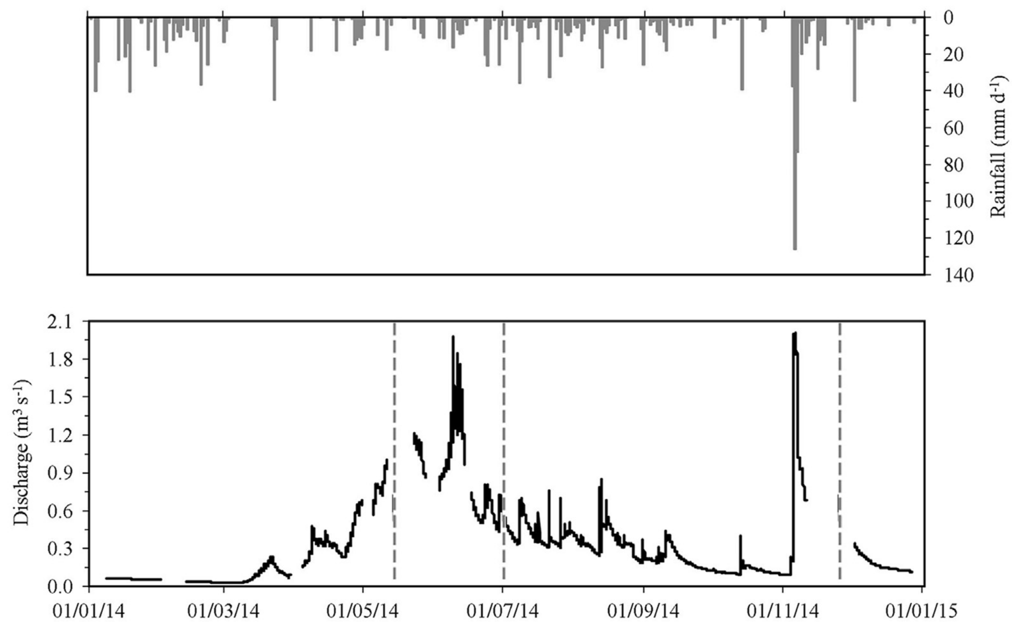

Fig. 3. Rainfall and discharge during 2014 (gaps in the discharge data are due to temporary malfunction of water level gauges). The grey dashed lines correspond to the PIT surveys.

Table 1
Main characteristics of monitored floods: R_{24} and R_{48} are the cumulative rainfall during the 24 and 48 h before the event, Q_{PEAK} is the peak of water discharge during the flood event, *RI* the recurrence interval, *ER* the effective runoff, *BL* and BL_r are the amount of bedload and transport rate, respectively, while D_{50} is the 50th percentile of grain size transported.

Flood	R_{24} (mm)	R_{48} (mm)	Q_{PEAK} ($m^3 s^{-1}$)	*RI* (years)	*ER* ($10^3 m^3$)	*BL* (m^3)	BL_r ($m^3 h^{-1}$)	D_{50} (mm)
May 2014	17.8	19.0	1.00	1.1	–	–	–	–
June 2014	16.6	16.6	2.06	1.7	16.6	65.6	4.7	41
November 2014	126.2	164.2	2.06	1.7	33.3	2.7	0.1	38

Table 2
Main characteristics of PIT surveys: Q_{PEAK} occurred during the monitored period, Li is the mean travel distance, n and n_m are the number of tracers detected and mobilized, respectively, while Rr is the recovery rate.

Survey	Q_{PEAK} ($m^3 s^{-1}$)	*Li* (m)	*n* (n)	n_m (n)	*Rr* (%)
May 2014	1.00	2.48	215	27	86
June 2014	2.06	117.03	192	101	77
November 2014	2.06	95.18	166	81	70

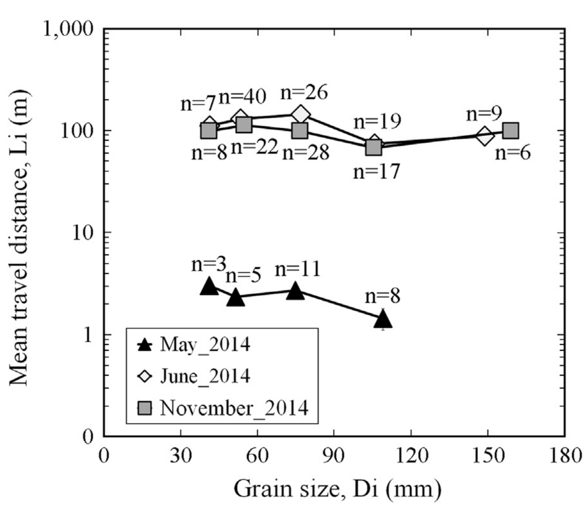

Fig. 4. Relation between mean travel distances and particle size classes, for the three events monitored.

the first phase of the snowmelt period, on May 11 with a Q_{PEAK} = 1.00 $m^3 s^{-1}$ (*RI* = 1.1 yr). Analysis of the antecedent rainfall showed that the runoff due to precipitation was limited, with R_{24} and R_{48} of 17.8 and 19 mm, respectively. Subsequently, there were two near-bankfull floods on June 9 and November 5 (Table 1). In both cases, the discharge peaked at 2.06 $m^3 s^{-1}$ with a *RI* of 1.7 years, but the events appear quite different in terms of runoff patterns. Due to the persistent snowmelt in 2014, the event on June 9 can be defined as a rain-on-snow event. The moderate rainfall recorded on June 9 (R_{24} = 16.6 mm) was concentrated in the afternoon, the rainfall-runoff thus, combined with the runoff provided by the intense snowmelt to yield the near-bankfull flow. Instead, the flood on November 5 was a typical autumn event triggered by heavy and persistent rainfall, as stressed by R_{24} and R_{48} of 126.2 and 164.0 mm, respectively (Table 1). To investigate the sediment mobility triggered by these events, post-flood PIT surveys were done (Fig. 3).

Significant recovery rates (i.e. tracers detected among the total population) were achieved during the three field surveys, with percentages from 70% in November to 86% in May (Table 2).

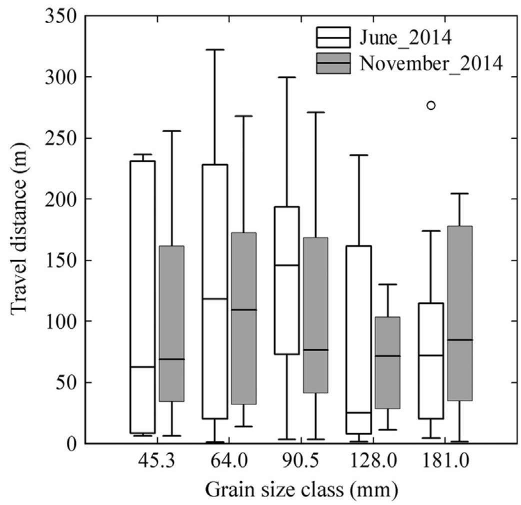

Fig. 5. Boxplot of the distribution of travel distances across grain size classes, for the near-bankfull events. The box limits indicate the 25th and 75th percentiles, the whiskers represent the non-outlier ranges, while the line within the box marks the median values. The circle indicates the outliers.

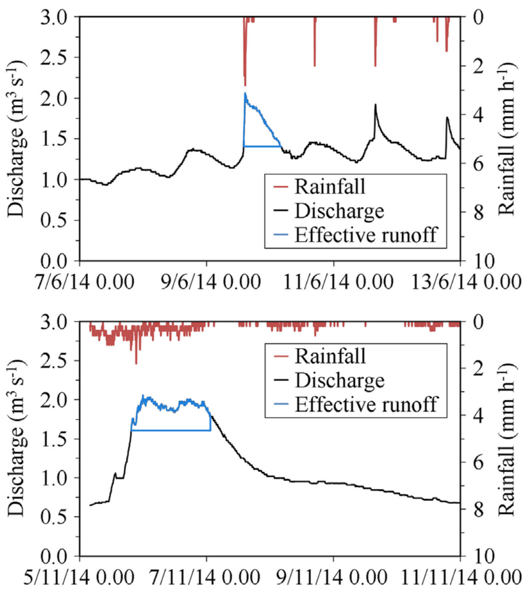

Fig. 6. Rainfall and discharge time series during June 2014 (A) and November 2014 (B) bedload events. The blue line indicates the Effective Runoff (*ER*).

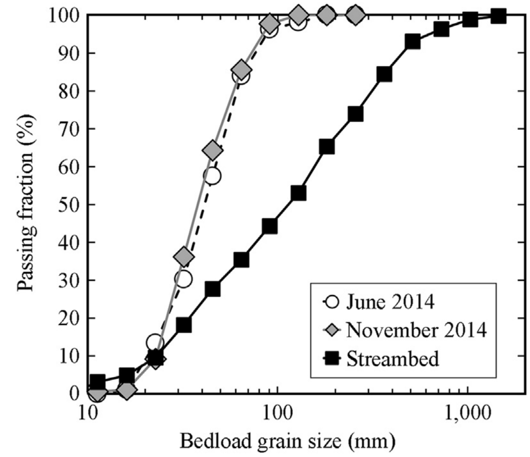

Fig. 7. GSD of streambed material compared to the bedload transported by the June 2014 and November 2014 events.

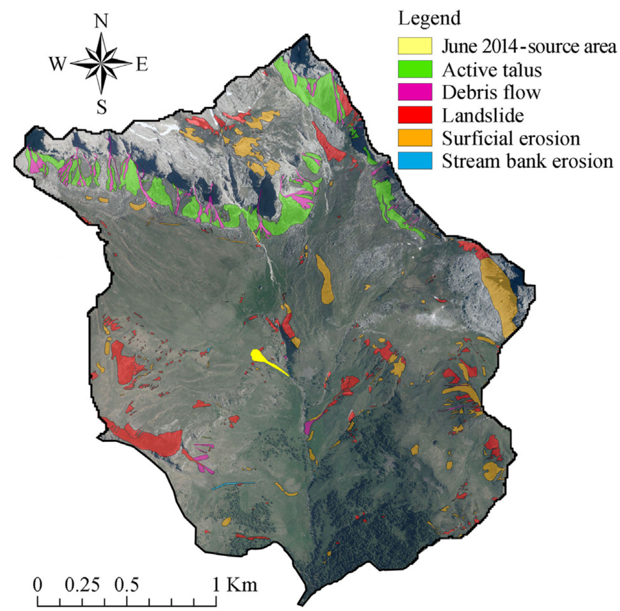

Fig. 8. Map of sediment sources detected in the Rio Cordon basin in 2006 (modified from Cavalli et al., 2016), updated with the source area of the June 2014 flood event.

Among the investigated events, a clear difference can be noted in terms of both tracers mobilized (n_m, displacement > 1 m) and travel distance. The number of PIT-tags mobilized was 101 by the June flood, 81 in November, and 27 in May. Similarly to the displacement, the mean travel distances (*Li*) triggered by the near-bankfull events, i.e. June and November, were 117.03 m and 95.18 m, respectively. The mean travel distance decreased by more than one order of magnitude in the below-bankfull event (i.e. May), reaching 2.48 m (Table 2). To investigate the effects triggered by the magnitude of the event on the grain size-displacement relation (*Di-Li*), the mobilized tracers were grouped by flood. Once grouped, the tracers were reclassified according to their *b-axis*, using the grain-size classes of 45.3, 64, 90.5, 128, and 181 mm, and the mean travel distance was then estimated for each particle size class. Fig. 4 shows the results of the *Di-Li* relation, highlighting the different magnitudes of displacement triggered.

The below-bankfull event (i.e. May) showed for all grain size classes that *Li* is constantly one order of magnitude lower than those of the near-bankfull floods (i.e. June and November). Moreover, the May flood caused exclusively the displacement of tracers with $D < 128$ mm. Instead, equal mobility conditions seem to have occurred during the events in June and November, with mobilization of the larger tracers (Fig. 4). In terms of the *Di-Li* relation, the near-bankfull events showed quite comparable behaviour. This similarity can be clearly observed comparing the travel distance covered by the grain size classes (Fig. 5). In the two near-bankfull events, the ranges of travel distance were similar, in particular in the 45.3, 64, and 181 mm classes, while displacements partly differed in the 90.5 and 128 mm classes.

Even if some grain was mobilized in all monitored events, only the near-bankfull events in June and November transported coarse material to the monitoring station, while no bedload flux was observed in the May flood. During the first bedload event, the water discharge peaked on June 9 at 2:40 PM with 2.06 m^3 s^{-1}. The bedload lasted for 14 h between 2:10 PM on June 9 and 4:10 AM

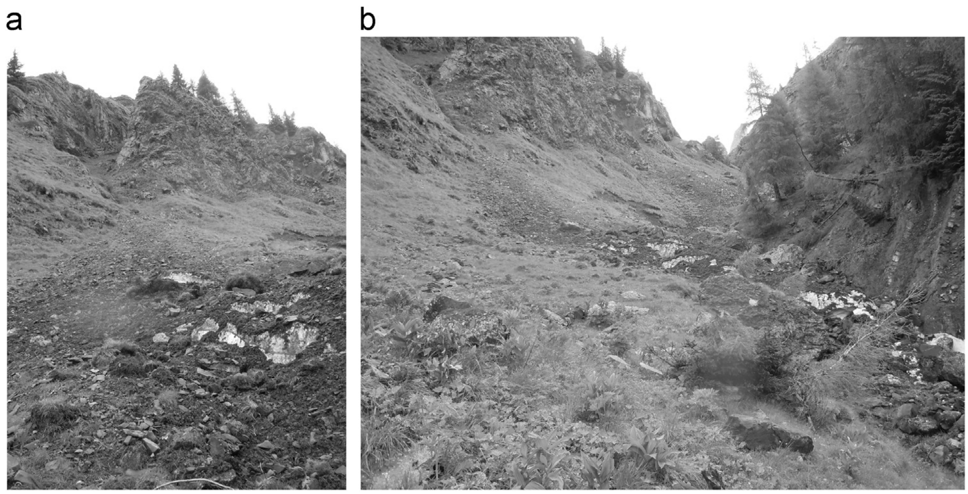

Fig. 9. Hillslope collapse that supplied material to the June 2014 bedload event, in figure B the stream flows from top to the bottom.

on June 10, beginning and ending with a discharge of approximately 1.4 m^3 s^{-1}. The effective runoff was thus 16.6 × 10^3 m^3, with a bedload yield of 65.6 m^3 (Fig. 6A).

Due to the considerable amount of transported sediments, the bedload transport rate (BL_r) also reached a significant value, equal to 4.7 m^3 h^{-1} (Table 1). The largest particle detected in the storage area had a *b-axis* = 230 mm. The material mainly consisted of coarse gravel (pebbles) with some small cobbles. Collecting 262 particles, the GSD percentiles were estimated. The D_{16}, D_{50}, D_{84}, and D_{90} were estimated as 16, 41, 64, and 76 mm, respectively (Fig. 7).

A debris flow channel located in the median part of the basin was identified as a source area (Fig. 8). Field evidence (i.e. traces of moved loam) suggested the occurrence of a debris flow in this area (Fig. 9).

The second bedload peaked on November 5, at 11:55 PM with a Q_{PEAK} = 2.06 m^3 s^{-1}. The bedload started at 1.6 m^3 s^{-1} (November 5 – 7:25 PM) and ended at 1.8 m^3 s^{-1} (November 7 – 1:10 AM), transporting 2.7 m^3 of sediment to the monitoring station storage area (Table 1). Overall, the bedload lasted for approximately 30 h with a bedload rate of 0.1 m^3 h^{-1}, while *ER* was 33.3 m^3 10^3 (Fig. 6B). As in the June bedload event, the material accumulated in the storage area was characterized in terms of GSD. A total of 174 particles were collected and measured by the grid by number method. The D_{16}, D_{50}, D_{84}, and D_{90} percentiles were 25, 38, 62, and 73 mm, respectively (Fig. 6). No active source area was detected during the post-flood survey for this event.

4. Discussion

In terms of Q_{PEAK}, the three floods investigated ranged between 1.00 and 2.06 m^3 s^{-1}, corresponding to RI = 1.1 (below-bankfull) to RI = 1.7 (near-bankfull). The results obtained from the bedload tracing highlighted a clear difference in sediment mobility among the events. First, the mean travel distance increases by more than one order of magnitude from the below-to near-bankfull floods (Fig. 4), suggesting that it is clearly related to the event magnitude. Focusing on the near-bankfull events (both Q_{PEAK} = 2.06 m^3 s^{-1}) a substantial similarity in terms of displacements can be observed comparing the travel distances of the grain size classes (Fig. 5). In this sense, Q_{PEAK} appears to better describe the travel distance-event magnitude relation than the other hydrological features (i.e. effective runoff). Regarding the grain size tracked, only a fraction of tracers ($D < 128$ mm) was mobilized by the below-bankfull event. Moreover, the displacement is lower in terms of both tracers mobilized and travel distance per grain size class (Fig. 4) compared to the near-bankfull events. During these floods, the *Di-Li* relation reveals that tracers experienced equal mobility conditions, in which the displacement appears unaffected by particle size. Furthermore, the entire range of grain sizes tracked was mobilized during the near-bankfull events.

Analyzing a range of Q_{PEAK} between 0.85 and 10.42 m^3 s^{-1}, and using colored particles and radiotracers to trace the bedload, Mao and Lenzi (2007) observed equal mobility conditions in the Rio Cordon only during floods with $RI > 5$, while size-selective transport prevailed during lower magnitude events. Despite the lower flood magnitude, a similar behavior was observed during the floods discussed here. As expected, the increase in flood magnitude led to a change from size-selective transport to equal mobility conditions. Interestingly, the equal mobility conditions observed here appear to be induced by lower hydraulic forcing than those observed previously in the Rio Cordon. The finer GSD tracked and different bedload tracing method could explain this result. If compared with the present work, Mao and Lenzi (2007) did their research on sediment mobility with a larger range of particle sizes. They used tracers with a diameter range between 32 and 512 mm, while in this study the range of *b-axis* is 40–190 mm. Nevertheless, the focus of this study on a finer fraction enabled it to be clearly observed that near-bankfull events could trigger equal mobility up to large cobbles. Additionally, the PIT-tags enhanced the quality and quantity of the sediment mobility data collected in the field, particularly as compared to colored particles and radiotracers. In contrast with these tracers, PIT-tags allow even local displacements to be clearly identified and permit buried PIT-tags to be detected, thereby increasing recovery rates (Rr = 70–86%). Overall, further analyses are required to better understand mobility in the Rio Cordon, but despite the short-term investigation, the results demonstrated that a large part of streambed material can be mobilized by near-bankfull events, also causing significant displacements ($Li > 100$ m). Further analysis could focus on the mobility of the coarser fraction of streambed material (i.e. boulders), to analyze the influence of the high degree of streambed armoring and bedforms on sediment mobility, and to determine the grain motion type and particle hop length (Sklar & Dietrich, 2004).

In the literature, only a few studies have analyzed flood events in steep streams relying on displacement of tracers and bedload magnitude (e.g., Lenzi, 2004; Schneider et al., 2014). Here, although all monitored events triggered mobility of the tracers, only the near-bankfull floods caused bedload to reach the monitoring station. These events appear similar, in terms of both Q_{PEAK}

and *Li*, while the bedload amount (*BL*) differs by one order of magnitude. Specifically, the June event transported 65.6 m^3, while barely 2.7 m^3 were transported during the November flood. In addition to Q_{PEAK}, even the antecedent rainfall (i.e. R_{24}, R_{48}) and *ER* appear to be poor descriptors for bedload magnitude, exhibiting a negative correlation. In fact, the R_{24} measured in the November flood (R_{24}=126.2 mm) was one order of magnitude higher than that during the 24 h preceding the June event (R_{24}=16.6 mm), while the hydrograph volume that contributed to the transport in November ($ER = 33.3 \times 10^3$ m^3) was roughly two-fold higher compared to June ($ER = 16.6 \times 10^3$ m^3). Interestingly, the R_{24} observed in the November flood is fully comparable to the rainfall ($R_{24} \approx$ 108.0 mm) recorded in the Rio Cordon area during the September 1994 exceptional event ($RI > 100$), which showed Q_{PEAK}=10.42 m^3 s^{-1} and $BL \approx$ 900 m^3 (Lenzi et al., 1999). Despite the similar 24-h cumulative value, the rainfall rates clearly differed. Indeed, the summer storm that triggered the September 1994 event featured maximum rates of 7.2 mm for 5-min and 25.3 mm for 30-min (Lenzi & Marchi, 2000), while the 5-, 30-, and 60-min rates recorded during the persistent November 2014 rainfall were merely 1.8, 5.2, and 7.0 mm, respectively. The rainfall rates in November 2014 are also lower than in June 2014, when 2.8 mm fell in 5-min, 11.0 mm in 30-min, and 15.0 mm in 60-min.

The different rates observed between the September 1994 and 2014 floods seem to partly explain the diverse sediment dynamics. Indeed, the Rio Cordon basin currently has clearly degraded sediment supply conditions compared to 1994, with most sediment source areas distant and not connected to the channel network (Fig. 8). Under these conditions, the bedload magnitude appears to relate better to the sediment supply than to the hydrological features (i.e. R_{24}, Q_{PEAK}, and *ER*). Indeed, the June bedload event was supplied by a large debris flow that occurred in the middle part of the basin (Fig. 8), while no field evidence was found subsequent to the November event. This suggests that the coarse material may have been provided by minor bank erosion or by loose material provided locally by hillslope collapses and mobilized by the increased water stage. The high transport efficiency observed in June could be explained by the type of sediment supply. Given the proximity of a specific source area to the channel network, the sediment connectivity appeared guaranteed, also thanks to the mixed nature of the supply. Indeed, the field evidence suggested that, in the debris flow channel identified as the source area, an avalanche was followed by a debris flow in June (Fig. 9). In light of this, the debris flow was likely triggered by the low-moderate rainfall in June (R_{24}=16.6 mm) acting on the only partially snow-covered source area.

In terms of grain sizes, the bedload transported to the monitoring station by the two near-bankfull floods appears quite similar, but clearly finer than the streambed material (Fig. 7). This result seems to be consistent with the concept of "traveling bedload" (Yu et al., 2009), which typically occurs in paved mountain streams when supplied by hillslopes processes. A local injection of sediment triggers bedload, but only the finer fraction is transported, not interacting with the armor layer and bedforms, while most coarser sediment is deposited on the channel bed (Schuerch et al., 2006). Although this process is particularly evident in the Rio Cordon, it is worth noting that also large cobbles (*b-axis*=230 mm), larger than the tracers installed and in line with the D_{75} (256 mm) of the streambed surface, were transported to the monitoring station by the June event. The results obtained from the investigation of the most recent bedload events support the hypothesis that high-frequency floods in the Rio Cordon exhibit high bedload transport rate only if supplied by hillslope processes (i.e. mud flow, debris flow), or if coupled with an active source area (Recking, 2012). Under the current supply-limited condition, with a highly paved streambed, traveling bedload appears to be the most significant transport process in the Rio Cordon.

5. Conclusions

In 2014, three high-frequency flood events were investigated in terms of both sediment mobility and bedload magnitude. Regarding the bedload tracing, there was a clear difference in terms of both number of tracers mobilized and mean travel distance. Unlike what was observed in higher magnitude floods, during the below-bankfull event only the fraction $D < 128$ mm of tracers were transported. In terms of mean displacement, the two near-bankfull events showed a substantial similarity with average travel distance one order of magnitude higher than that in the below-bankfull event. Additionally, significant evidence of equal mobility conditions was observed as a consequence of the near-bankfull events, when sediment mobility appeared unaffected by particle size.

Compared to the other hydrological features, Q_{PEAK} proved to be the best descriptor for mean displacement. The obtained results from the PIT-tags highlighted that a near-bankfull event may strongly influence sediment displacement and consequently mobilize a large part of the streambed material for long distances. Despite the tracers mobility observed, only the near-bankfull events caused bedload transport to reach the monitoring station. In terms of Q_{PEAK}, these events are fully comparable (both Q_{PEAK}=2.06 m^3 s^{-1}), while the bedload differs by more than one order of magnitude (i.e. 65.6 vs. 2.7 m^3). These results suggest that in the Rio Cordon, under the current supply-limited condition and strong armored layer, the hydrological features of the event (i.e. R_{24}, Q_{PEAK}, and *ER*) are not the most relevant descriptors for the bedload amount. In the light of the existing conditions and in the absence of an exceptional flood able to alter the sediment dynamics, the high frequency events appear to have significant bedload only if coupled with and supplied by an active source area. In recent years hillslope processes were the main active sources supporting such a hypothesis.

This study also demonstrated that, once supplied by coarse particles, the Rio Cordon can easily mobilize a large amount of material. In this sense, the mobility of large boulders as well as the influence of a paved streambed and bedforms on the entrainment mobility are issues to be further explored. Indeed, only a few field datasets are available in the literature in which both the bedload magnitude and travel distance of tracers were investigated in steep streams. Notwithstanding the short time scale, this study is an attempt in this direction, focusing particularly on the comparison of flood events with apparently similar magnitude but clearly different sediment dynamics.

Acknowledgments

This research was supported by the University of Padova Research Projects 'Sediment Transfer Processes in an Alpine Basin: Sediment Cascades from Hillslopes to the Channel Network-BIRD167919', 'WoodAlp: Linking Large Wood and Morphological Dynamics of Gravel Bed Rivers of Eastern Italian Alps-PRAT-CPDA149091', and 'Relationship between Sediment Transport, Riparian Vegetation and Large Wood along a Gravel Bed River: the Piave River Study Case (North-East Italy)-DOR1695175'. We would like to thank Prof. Mario Aristide Lenzias the article has benefited from discussion with him as well as Emanuel Rigon, Johnny Moretto, Diego Ravazzolo, and Fabio Delai for their help in the field surveys. We would also like to thank Alison Garside for revising the English, and many thanks go to Matteo Cesca and Walter Testor for technical support. We are grateful to the Associate Editors (Markus Noack and Charles Steven Melching) and three anonymous reviewers for their constructive comments, which helped us to improve the manuscript.

References

Ashworth, P. J., & Ferguson, R. I. (1989). Size-selective entrainment of bed load in gravel bed streams. *Water Resources Research*, *25*(4), 627–634.

Baewert, H., & Morche, D. (2014). Coarse sediment dynamics in a proglacial fluvial system (Fagge River, Tyrol). *Geomorphology*, *218*, 88–97.

Bathurst, J. C. (2013). Critical conditions for particle motion in coarse bed materials of nonuniform size distribution. *Geomorphology*, *197*, 170–184.

Bathurst, J.C., Graf, W.H., & Cao, H.H. (1983). Initiation of sediment transport in steep channels with coarse bed material. In B. Mutlu Sumer & A. Müller (eds.), *Mechanics of Sediment Transport.* Proceedings of Euromech 156. Istanbul, July 1982, 207–213.

Beylich, A. A., & Laute, K. (2015). Sediment sources, spatiotemporal variability and rates of fluvial bedload transport in glacier-connected steep mountain valleys in western Norway (Erdalen and Bødalen drainage basins). *Geomorphology*, *228*, 552–567.

Bunte, K., Abt, S. R., Potyondy, J. P., & Swingle, K. W. (2008). A comparison of coarse bedload transport measured with bedload traps and Helley–Smith samplers. *Geodinamica Acta*, *21*(1/2), 53–66.

Cavalli, M., Tarolli, P., Dalla Fontana, G., & Marchi, L. (2016). Multi-temporal analysis of sediment source areas and sediment connectivity in the Rio Cordon catchment (Dolomites). *Rendiconti Online Società Geologica Italiana*, *39*, 27–30.

Cavalli, M., Trevisani, S., Comiti, F., & Marchi, L. (2013). Geomorphometric assessment of spatial sediment connectivity in small Alpine catchments. *Geomorphology*, *188*, 31–41.

Dell'Agnese, A., Brardinoni, F., Toro, M., Mao, L., Engel, M., & Comiti, F. (2015). Tracing bedload transport in a high-elevation, formerly-glaciated mountain basin. *Earth Surface Dynamics*, *3*, 527–542.

Downs, P. W., Soar, P. J., & Taylor, A. (2016). The anatomy of effective discharge: The dynamics of coarse sediment transport revealed using continuous bedload monitoring in a gravel-bed river during a very wet year. *Earth Surface Processes and Landforms*, *41*(2), 147–161.

Fattorelli, S., Keller, H. M., Lenzi, M. A., & Marchi, L. (1988). An experimental station for the automatic recording of water and sediment discharge in a small alpine watershed. *Hydrological Sciences Journal*, *33*(6), 607–617.

Ferguson, R. I., & Wathen, S. J. (1998). Tracer-pebble movement along a concave river profile: Virtual velocity in relation to grain size and shear stress. *Water Resources Research*, *34*(8), 2031–2038.

Fraley, L. (2004). *Methods of measuring fluvial sediment. Center for urban environment research and education*. Baltimore: University of Maryland.

Habersack, H., Kreisler, A., Rindler, R., Aigner, J., Seitz, H., Liedermann, M., & Laronne, J. B. Integrated automatic and continuous bedload monitoring in gravel bed rivers. *Geomorphology*, http://dx.doi.org/10.1016/j.geomorph.2016.10.020.

Hammond, F. D. C., Heathershaw, A. D., & Langhorne, D. N. (1984). A comparison between Shields' threshold criterion and the movement of loosely packed gravel in a tidal channel. *Sedimentology*, *31*(1), 51–62.

Houbrechts, G., Levecq, Y., Peeters, A., Hallot, E., van Campenhout, J., Denis, A., & Petit, F. (2015). Evaluation of long-term bedload virtual velocity in gravel-bed rivers (Ardenne, Belgium). *Geomorphology*, *251*, 6–19.

Krein, A., Schenkluhn, R., Kurtenbach, A., Bierl, R., & Barrière, J. (2016). Listen to the sound of moving sediment in a small gravel-bed river. *International Journal of Sediment Research*, *31*(3), 271–278.

Lamarre, H., MacVicar, B., & Roy, A. G. (2005). Using passive integrated transponder (PIT) tags to investigate sediment transport in gravel-bed rivers. *Journal of Sedimentary Research*, *75*, 736–741.

Lamb, M. P., Dietrich, W. E., & Venditti, J. G. (2008). Is the critical Shields stress for incipient sediment motion dependent on channel-slope? *Journal of Geophysical Research: Earth Surface*, *113*(2), F02008.

Lenzi, M. A. (2004). Displacement and transport of marked pebbles, cobbles and boulders during floods in a steep mountain stream. *Hydrological Processes*, *18*(10), 1899–1914.

Lenzi, M. A., D'Agostino, V., & Billi, P. (1999). Bedload transport in the instrumented catchment of the Rio Cordon: Part I: Analysis of bedload records, conditions and threshold of bedload entrainment. *Catena*, *36*(3), 171–190.

Lenzi, M. A., Mao, L., & Comiti, F. (2003). Interannual variation of suspended sediment load and sediment yield in an Alpine catchment. *Hydrological Sciences Journal*, *48*(6), 899–915.

Lenzi, M. A., Mao, L., & Comiti, F. (2006a). Effective discharge for sediment transport in a mountain river: Computational approaches and geomorphic effectiveness. *Journal of Hydrology*, *326*(1-4), 257–276.

Lenzi, M. A., Mao, L., & Comiti, F. (2006b). When does bedload transport begin in steep boulder-bed streams? *Hydrological Processes*, *20*, 3517–3533.

Lenzi, M. A., & Marchi, L. (2000). Suspended sediment load during floods in a small stream of the Dolomites (northeastern Italy). *Catena*, *39*, 267–282.

Liébault, F., Bellot, H., Chapuis, M., Klotz, S., & Deschâtres, M. (2012). Bedload tracing in a high-sediment-load mountain stream. *Earth Surface Processes and Landforms*, *37*, 385–399.

Liébault, F., Jantzi, H., Klotz, S., Laronne, J. B., & Recking, A. (2016). Bedload monitoring under conditions of ultra-high suspended sediment concentrations. *Journal of Hydrology*, *540*, 947–958.

Liébault, F., & Laronne, J. B. (2008). Evaluation of bedload yield in gravel-bed rivers using scour chains and painted tracers: The case of the Esconavette Torrent (southern French Prealps). *GeodinamicaActa*, *21*(1), 23–34.

Mao, L., Carrillo, R., Escauriaza, C., & Iroume, A. (2016). Flume and field-based calibration of surrogate sensors for monitoring bedload transport. *Geomorphology*, *253*, 10–21.

Mao, L., & Lenzi, M. A. (2007). Sediment mobility and bedload transport conditions in an Alpine stream. *HydrologicalProcesses*, *21*, 1882–1891.

Mao, L., Uyttendaele, G. P., Iroumé, A., & Lenzi, M. A. (2008). Field based analysis of sediment entrainment in two high gradient streams located in Alpine and Andine environments. *Geomorphology*, *93*, 368–383.

Olinde, L., & Johnson, J. P. L. (2015). Using RFID and accelerometer-embedded tracers to measure probabilities of bed load transport, step lengths, and rest times in a mountain stream. *Water Resources Research*, *51*, 7572–7589.

Picco, L., Mao, L., Rigon, E., Moretto, J., Ravazzolo, D., Delai, F., & Lenzi, M. A. (2012). *An update of the magnitude-frequency analysis of Rio Cordon (Italy) bedload data after 25 years of monitoring*, *356*. *IAHS Publication* (ISSN: 0144-7815).

Rainato, R., Mao, L., Garcia-Rama, A., Picco, L., Cesca, M., Vianello, A., & Lenzi, M. A. Three decades of monitoring in the Rio Cordon instrumented basin: Sediment budget and temporal trend of sediment yield. *Geomorphology*, http://dx.doi.org/10.1016/j.geomorph.2016.03.012, in press.

Recking, A. (2012). Influence of sediment supply on mountain streams bedload transport. *Geomorphology*, *175-176*, 139–150.

Rickenmann, D., Turowski, J. M., Fritschi, B., Klaiber, A., & Ludwig, A. (2012). Bedload transport measurements at the Erlenbach stream with geophones and automated basket samplers. *Earth Surface Processes and Landforms*, *37*, 1000–1011.

Schneider, J. M., Turowski, J. M., Rickenmann, D., Hegglin, R., Arrigo, S., Mao, L., & Kirchner, J. W. (2014). Scaling relationships between bed load volumes, transport distances, and stream power in steep mountain channels. *Journal of Geophysical Research: Earth Surface*, *119*, 533–549.

Schuerch, P., Densmore, A. L., McArdell, B. W., & Molnar, P. (2006). The influence of landsliding on sediment supply and channel change in a steep mountain catchment. *Geomorphology*, *78*, 222–235.

Schwendel, A. C., Death, R. G., Fuller, I. C., & Tonkin, J. D. (2011). A new approach to assess bed stability relevant for invertebrate communities in upland streams. *River Research and Applications*, *28*, 1726–1739.

Sklar, L. S., & Dietrich, W. E. (2004). A mechanistic model for river incision into bedrock by saltating bed load. *Water Resources Research* (p. *40*), *40*. http://dx.doi.org/10.1029/2003WR002496.

Vazquez-Tarrio, D., & Menendez-Duarte, R. (2014). Bedload transport rates for coarse-bed streams in an Atlantic region (Narcea River, NW Iberian Peninsula). *Geomorphology*, *217*, 1–14.

Wohl, E. (2015). Particle dynamics: The continuum of bedrock to alluvial river segments. *Geomorphology*, *241*, 192–208.

Yager, E. M., Kenworthy, M., & Monsalve, A. (2015). Taking the river inside: Fundamental advances from laboratory experiments in measuring and understanding bedload transport processes. *Geomorphology*, *244*, 21–32.

Yu, G., Wang, Z., Zhang, K., Chang, T., & Liu, H. (2009). Effect of incoming sediment on the transport rate of bed load in mountain streams. *International Journal of Sediment Research*, *24*, 260–273.